Acta Cryst. (1975). B31, 1797

The Crystal Structure of a Boron-Rich Boron Carbide*†

BY HARRY L. YAKEL

Oak Ridge National Laboratory, Oak Ridge, Tennessee 37830, *U.S.A.*

(*Received* 20 *November* 1974; *accepted* 3 *February* 1975)

Structural changes accompanying extreme boron-enrichment of boron carbide were deduced with Mo $K\alpha$ X-ray diffraction data obtained from a twinned aggregate containing a minimal amount of carbon. The crystal system remains rhombohedral, probable space group $R\bar{3}m$, as for B_4C, but unit-cell parameters show significant expansions compared to those of a 20 at.% C material. Fourier, difference Fourier, and least-squares calculations produced a final weighted R value of 9·04% and a σ_1 of 0·985 for a structure that retains (B_{12}) icosahedra and randomly replaces about one fourth of the [CBC] chains with [B_4] groups. Terminal atoms of the latter are fixed along a threefold axis and have fivefold coordination, being bonded to two central (or bridge) atoms of the group and to three icosahedral atoms. Bridge atoms lie in two of twelve equivalent positions near a plane normal to the threefold axis; they also have fivefold coordination, being bonded to the two terminal atoms of the group and to three icosahedral atoms. The chemical composition of the proposed structure, 9·7 at.% C, agrees with published phase diagrams, but exceeds the analyzed carbon contents of 4·8 at.% C (bulk chemical analysis) and 8 at.% C (ion microprobe analysis). Possible reasons for the location of the boron-rich terminus of the boron carbide phase field are discussed in view of the proposed structure.

I. Introduction

Many problems remain unanswered concerning the physical and structural chemistry of the phase (or phases) known as boron carbide. In summarizing the situation, Elliott (1961) noted reports of a single phase with carbon solubility limits varying from a minimum of 4–9 at.% C to a maximum of 20–28 at.% C, as well as reports of two or more phases within similar limits. The diagram determined by Elliott from metallographic, X-ray diffraction, and thermal analytical data shows a single phase in the solubility range from 9 to 20 at.% C, with a congruent melting point of 2450°C at 18·5 at.% C.

The crystal structure of an equilibrium boron carbide was first derived by Zhdanov & Sevast'yanov (1941) and by Clark & Hoard (1943). Working with a crystal of composition near the carbon-rich extreme of the phase field, the latter authors found a rhombohedral unit cell (space group $R\bar{3}m$), with $a^R = 5{\cdot}19$ Å and $\alpha^R = 65{\cdot}3°$, containing 15 atoms. Of these, 12 (assumed to be boron) were located at the vertices of a nearly regular icosahedron described by two sets of crystallographically distinct positions with point symmetry m. Three (assumed to be carbon) formed a linear chain, or intericosahedral linking component, along the threefold axis. Icosahedra were centered on lattice points which would constitute a face-centered cubic array were $\alpha = 60°$. Each icosahedral atom formed five intraicosahedral bonds and one external bond; half [B(2) or rhombohedral boron atoms] used this external bond to link with other isosahedra, while the other half [B(1) or equatorial boron atoms] used this bond to link with terminal atoms of chains.

About 20 years after this initial description, Hoard & Hughes (1967) mentioned X-ray diffraction work then in progress which suggested that central atoms of chains might not be carbon but boron. Later neutron and X-ray scattering studies of B_4C confirmed this refinement of the original arrangement (Walters & Green, 1970; Larson & Cromer, 1972, hereinafter LC). To achieve a proper chemical composition one must further assume the average substitution of a carbon for a boron atom in each icosahedron. Careful analyses of X-ray diffraction data have shown that this substitution occurs preferentially in rhombohedral sites (Larson, 1974). An average of recently reported lattice constants for boron carbides with about 20 at.% C is $a^R = 5{\cdot}165 \pm 0{\cdot}003$ Å, $\alpha^R = 65{\cdot}70 \pm 0{\cdot}05°$.

If B_4C is to be considered as a selective substitutional solid solution based on the ideal composition and crystal structure of $B_{13}C_2$, *i.e.*, rhombohedral (B_{12}) [CBC],† how does this structure accommodate compositions with 3 or 4 at.% C *less* than the ideal? Answers to this question have been proposed but must remain speculative in the absence of crystal structure

* Research sponsored by the U. S. Atomic Energy Commission under contract with the Union Carbide Corporation.

† A complete description of this work has been deposited with the British Library Lending Division as Supplementary Publication No. SUP 30928 (64 pp., 2 microfiches). Copies may be obtained through The Executive Secretary, International Union of Crystallography, 13 White Friars, Chester CH1 1NZ, England.

† In structural formulas for boron carbides, atoms comprising an average icosahedron will be written first within parentheses. This will be followed by a linear array of atoms enclosed in square brackets representing the average linking component configuration(s). Interstitial atoms, if any, will be written last in parentheses with subscript *i*. The total formula will thus correspond to the contents of an average rhombohedral unit cell.

analyses based on diffraction data from low-carbon boron carbides prepared under conditions approaching thermodynamic equilibrium. In this paper, I present results of such a determination together with possible solutions to some problems of variable composition in the single-phase field.

II. Preparation and preliminary analyses of material

The specimen whose structure will be described came from one of a series of samples prepared with varying B:C ratios. Details of the preparation are described in the more complete deposited version of this paper. Chemical analyses of a part of the specimen gave 5·3 wt% total carbon and 93·7 wt% total boron. X-ray diffraction powder patterns from a crushed portion of the product showed reflections from a rhombohedral boron carbide phase.

The small amount of material remaining after removal of the analytical and powder diffraction specimens was examined optically in the hope that useful single crystals could be found. Although no fragments larger than 0·1 mm were observed, and although twinning was indicated in all the larger fragments, a few showing reasonably good facial development were selected and mounted for further X-ray diffraction experiments.

Weissenberg photographs of these specimens, exposed with nickel-filtered Cu $K\alpha$ X radiation, confirmed the twinning apparent optically; the twin axis was a $\langle 011 \rangle_{\text{Rhomb}}$ direction. No systematic reflection absences were observed (rhombohedral indexing), and the diffracted intensities were qualitatively similar to those produced by B_4C. Two measurements of the density of the largest fragment by a flotation technique gave 2·455 and 2·457 g cm^{-3}.

III. Collection of X-ray diffraction data

The fragment whose density had been measured was positioned on an arc-less goniometer head and aligned at the center of a computer-controlled Picker four-circle diffractometer. For the first data collection, a copper-target X-ray tube was used.

Photographic data for this fragment had shown that, in addition to the major lattice orientation, only one twin-related minor orientation was present. Iterated least-squares fits of measurements of 12 high-angle ($2\theta > 130°$) reflections from the major orientation were used to refine lattice and orientation parameters. The unit-cell constants were: $a^R = 5{\cdot}2065$ (1) Å, $\alpha^R = 66{\cdot}010$ (1)°, $V^R = 112{\cdot}733$ (6) Å^3, $M^R = 166{\cdot}8$ (1) a.m.u., $a^H = 5{\cdot}6720$ (1) Å, $c^H = 12{\cdot}1428$ (2) Å, $c^H/a^H = 2{\cdot}1408$ (1) (λ Cu $K\alpha = 1{\cdot}54178$ Å).

A complete set of nickel-filtered Cu $K\alpha$ diffraction data for both major and minor lattice orientations was collected in the $(\theta, 2\theta)$ scan mode to a maximum scattering angle of 160°. Within the precision of the measurements, the Laue group was $\bar{3}m$. All 111 independent reflections within the (0–160°) 2θ Cu $K\alpha$ limiting sphere were observed at least twice for each orientation. Integrated intensities were corrected for Lorentz, polarization, and absorption effects. Each of the independent reflections had an F^2 value greater than four times the estimated error of measurement.

The Mo $K\alpha$ data collection was made with the same specimen used for the Cu $K\alpha$ experiment. Diffracted intensities from the major orientation only were recorded in the $(\theta, 2\theta)$ scan mode to a maximum scattering angle of 160°. After elimination of reflections likely to be affected by interferences from the twin-related orientation, it still proved possible to measure intensities for at least one equivalent of each of the 971 independent reflections in the (0–160°) 2θ Mo $K\alpha$ limiting sphere. Again, the data were consistent with Laue group $\bar{3}m$ within experimental error.

The 6504 individual intensity measurements were corrected for Lorentz, polarization, and absorption effects. Replicate and equivalent reflections were averaged including an adjustable scale factor relating intensities of reflections produced from both orientations simultaneously with intensities of equivalent reflections produced from the major orientation only. About two thirds of the 971 independent Mo $K\alpha$ reflections had F^2 values greater than or equal to twice the estimated error of measurement, while slightly less than half had F^2 greater than or equal to four times that error. The Mo $K\alpha$ data set thus included many relatively imprecise observations – a consequence of the small size of the diffraction specimen and the limitations imposed by reasonable experimental data collection times.

IV. Structure determination

The starting point for analyses of both Cu $K\alpha$ and Mo $K\alpha$ data was the B_4C structure. This seemed justified in view of the similarity between diffracted intensities produced by boron-rich specimens and those recorded from B_4C crystals. The strategy of the analyses was based on the expectation that structural changes accompanying carbon depletion would become evident through iterated least-squares, Fourier, and difference Fourier calculations.

In the initial model, icosahedral boron atoms, B(1) and B(2), were located in two sets of positions 18(h) ($x, -x, z$; *etc.*), point symmetry m, of space group $R\bar{3}m$ referred to hexagonal axes. Values of x and z were $-0{\cdot}164$ and $0{\cdot}359$ for B(1) atoms and $-0{\cdot}106$ and $0{\cdot}113$ for B(2) atoms. Terminal carbon atoms, C(4), of chains were in positions 6(c) ($0,0,z$; *etc.*), point symmetry $3m$, with z equal to 0·383; while boron atoms, B(3), at chain centers were constrained to positions 3(b) ($0,0,\frac{1}{2}$; *etc.*), point symmetry $\bar{3}m$. All sites were fully occupied. Atomic scattering factors were those computed by Cromer & Waber (1964) from relativistic Dirac–Slater wave functions.

The fact that the Cu $K\alpha$ data were not sufficient to

yield an adequate solution to the detailed structure quickly became apparent and led to the Mo $K\alpha$ data acquisition. Nevertheless, analyses of the Cu $K\alpha$ results did indicate several important departures from the starting model that were to be confirmed by later work. They are fully described in the deposited version of this paper and may be summarized as follows:

(*a*) Normal (B_{12}) icosahedra.

(*b*) No interstitial atoms along threefold axes at positions suggested by Clark & Hoard (1943).

(*c*) Partial replacement of [CBC] chains by a configuration consisting of terminal boron atoms bridged by some number of boron atoms located on twofold axes perpendicular to a vacant central atom site.

Three cycles of full-matrix least-squares refinement of the unaltered starting model using all 971 independent Mo $K\alpha$ reflection averages yielded measures of agreement listed in Table 1 for model IM. The residual function minimized was $\sum w_{obs}(F^2_{obs}-S^2F^2_{calc})^2$. Here, w_{obs}, the weight of F^2_{obs}, was taken as $1/\sigma^2(F^2_{obs})$, where the variance $\sigma^2(F^2_{obs})$ included an empirical factor $(0{\cdot}03F^2_{obs})^2$ added to the statistical variance. Adjustments were computed for 5 positional parameters, 12 coefficients of anisotropic temperature factors, and one scale factor, S. An F_{obs} Fourier section normal to the hexagonal a_1 axis at $x=\frac{1}{2}$ was computed with phases for all reflections assigned on the basis of this refinement (Fig. 1). The map confirms the general structural changes inferred from the Cu $K\alpha$ data analysis and further suggests that terminal atoms of the configuration occasionally replacing [CBC] chains are definitely displaced from the C(4) position of the normal chain.

Table 1. *Agreement indices of trial models*

Definitions of these indices are the standard ones used by crystallographers. See Brown & Chidambaram (1969), for example, for specific equations.
Values without parentheses are computed for all reflections. Values in parentheses are computed for reflections with $F^2_{obs}>\sigma(F^2_{obs})$.

Model	$R(F)$	$R(F^2)$	$R_w(F^2)$	σ_1
IM	0·1348	0·1366	0·2048	2·204
	(0·1133)	(0·1309)	(0·2018)	(2·388)
MM	0·0968	0·0843	0·1265	1·364
	(0·0772)	(0·0802)	(0·1244)	(1·477)
FM	0·0849	0·0645	0·0904	0·985
	(0·0655)	(0·0605)	(0·0877)	(1·055)

With boron atoms at B(3) sites allowed a variable occupancy $A<1$, with carbon atoms at C(4) given an occupancy factor of A and a variable z initially set at 0·384, and with boron atoms at B(5), (0,0,z; *etc.*), given an occupancy factor of $(1-A)$ and a variable z initially set at 0·414, six least-squares cycles produced markedly improved measures of agreement (model MM, Table 1). The refined value of the single variable occupation parameter, $A=0{\cdot}748\pm0{\cdot}008$, was in reasonable accord with the peak densities of Fig. 1.

An $(F_{obs}-F'_{calc})$ partial difference Fourier was summed with F'_{calc} computed for all atoms but B(5) using parameters given by the final least-squares cycle

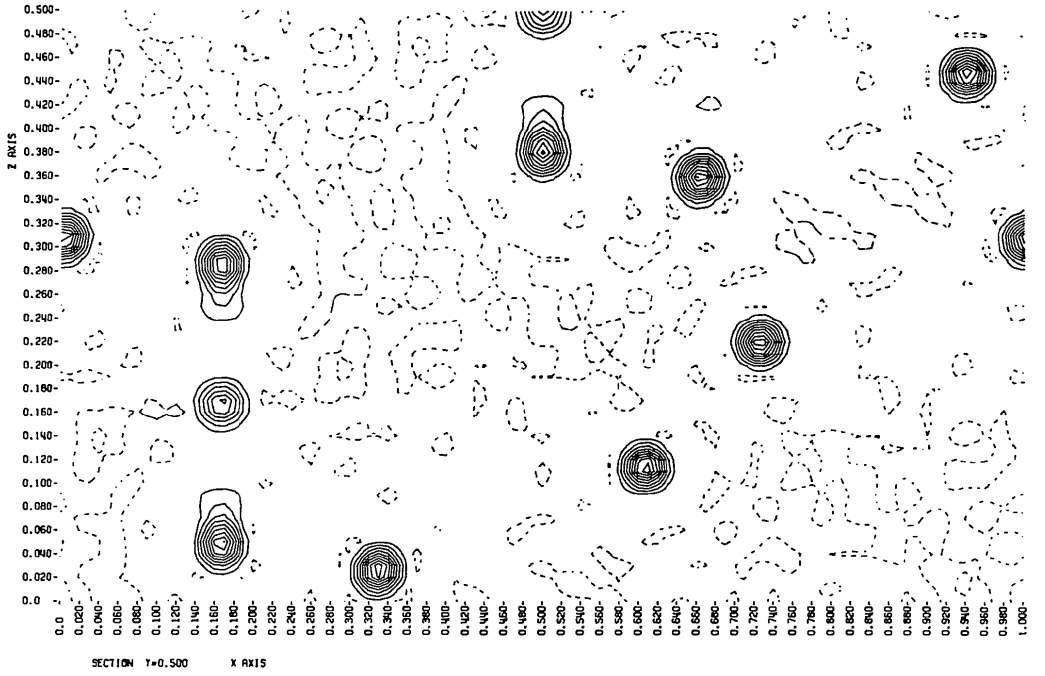

Fig. 1. An F_{obs} Fourier section normal to the hexagonal a_1 axis at $x=\frac{1}{2}$ prepared from the 971 independent Mo $K\alpha$ reflection data phased by a least-squares refinement of the starting model, (B_{12}) [CBC]. Coordinates refer to an alternate monoclinic cell defined by the vector equations: **a**(mon.) $=-\mathbf{a}_1$ (hex.) $-2\mathbf{a}_2$ (hex.); **b**(mon.) $=\mathbf{a}_1$ (hex.); **c**(mon.) $=$ **c**(hex.). Contours are drawn at intervals of 5·8 e Å^{-3} and negative contours are dashed.

of this five-atom refinement. The largest maxima in this map were associated with B(5) atoms; peak densities were 12·9 e Å^{-3}. The next largest maxima (1·6 e Å^{-3}) were all located in the $(x,y,\frac{1}{2})$ section which is reproduced in Fig. 2. These maxima correspond to partial occupation of general positions 36(i) (x,y,z; *etc.*) with $x=0{\cdot}26$, $y=0{\cdot}04$, and $z=0{\cdot}5$.

Randomly distributing the same number of boron atoms as were located in B(5) sites in this general B(6) site again produced significant improvements in measures of agreement after three least-squares cycles (model FM, Table 1). The group replacing the [CBC] chain is thus [B_4], containing two B(5) and two B(6) atoms. Parameters of this model are listed in Table 2. A complete (F_{obs}–F_{calc}) difference Fourier summed with the results of the final cycle showed positive maxima at (0,0,z; *etc.*), $z=0{\cdot}21$, with peak density 1·4 e Å^{-3}, and a series of maxima in the $z=\frac{1}{2}$ plane with peak heights of 0·5 to 0·7 e Å^{-3}. The latter are at the same positions as the secondary maxima in Fig. 2, while the former are close to the interstitial sites originally proposed by Clark & Hoard (1943). Attempts to further augment the model by adding a small number of boron atoms at these positions were unsuccessful in that no significant improvements in measures of agreement were produced and physically unreal temperature factor coefficients occurred for one or more atoms.

Other variations in model FM were made in an effort to improve the measures of agreement while maintaining physical reality, but none tested achieved that goal. Included were: application of extinction corrections to the observed data, addition of variable coefficients of third-rank thermal motion tensors for all atoms, lowering of the space group symmetry by elimination of mirrors ($R32$) or twofold axes ($R3m$), variation of occupation parameters of atoms at sites B(3), C(4), B(5), and B(6) with all other parameters fixed, and admixtures of variable numbers of boron and carbon atoms at these four sites.

A comment concerning the apparent impasse in elaborating model FM is in order. Descriptions of thermal motions in terms of Gaussian probability density functions and the use of atom scattering factors derived from spherical electron distributions are doubtlessly unrealistic and might be improved upon. On the other hand, although R values for model FM are about twice as large as might be expected for a precise structure determination, the standard deviation of an observation of unit weight, σ_1, is close to unity. Therefore the refinement may indeed be stretched to its ultimate limit, given the degree of imprecision of the Mo $K\alpha$ data set. A comparison of observed structure factors and those computed from model FM is given in the deposited paper.

V. Agreement of the refined structure with other physical measurements

The mass per rhombohedral unit cell resulting from model FM agrees with the value computed from the experimentally determined crystal density and unit-

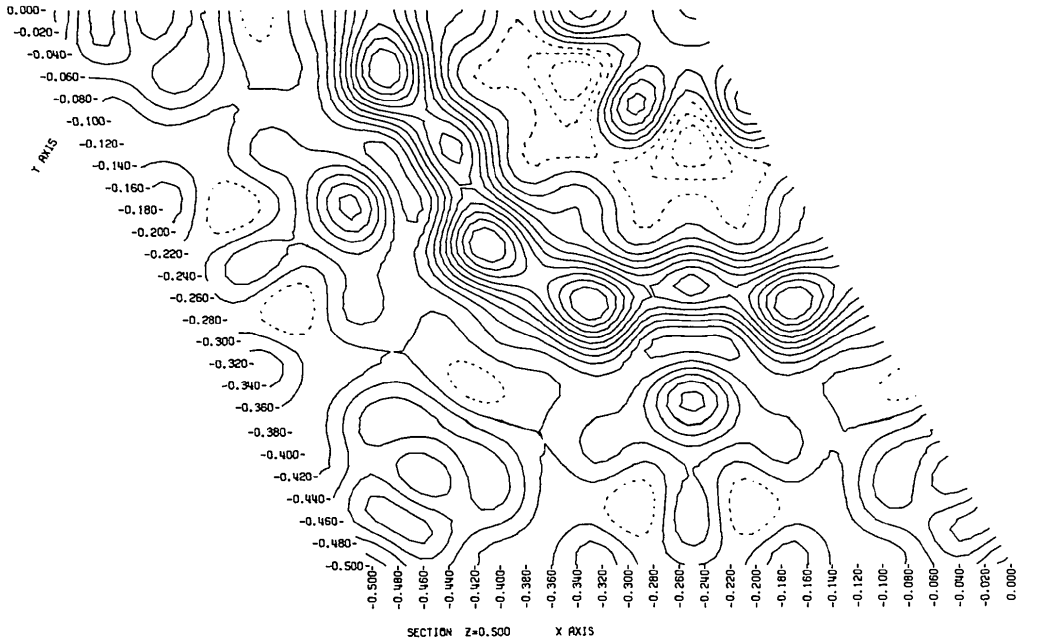

Fig. 2. A partial difference Fourier section normal to the hexagonal c axis at $z=\frac{1}{2}$ prepared from the 971 independent Mo $K\alpha$ reflection data phased by a least-squares refinement of the five-atom model (model MM, Table 1). Contributions of all atoms but B(5) have been subtracted from F_{obs} to give the Fourier coefficients. Contours are drawn at intervals of 0·17 e Å^{-3} and negative contours are dashed.

cell dimensions to the precision of the measurements involved. The chemical composition of the model, however, is $9{\cdot}72 \pm 0{\cdot}06$ at.% C which is significantly above the analyzed chemical composition of 4·84 at.% C for the bulk specimen.* Reasons for this discrepancy could include (1) biased errors introduced in the structural analysis, (2) biased errors introduced in the chemical analysis, and (3) compositional inhomogeneities in the bulk sample.

In the absence of any clear suggestions of error in the first two areas, experiments were performed to test the validity of the third possible reason for the composition discrepancy. Well exposed (72 hr) Cr $K\alpha$ Debye–Scherrer powder photographs of a crushed remnant of the bulk sample showed weak, broad maxima that could be ascribed to poorly crystallized β-rhombohedral boron (Sands & Hoard, 1957), a few sharper reflections that could not be identified, and the reflections of the major boron carbide phase. Microscopic examination of large intergrown aggregates showed surface textures that might indicate epitaxic formation of boron crystallites. Finally, the fragment used for the X-ray structural studies was broken from its mount and subjected to ion-microprobe analysis. This technique determines atomic species at surfaces by ejecting atoms with a beam of energetic nitrogen ions, then analyzing the sputtered atoms in a mass spectrometer (Evans, 1972). The ion beam may be focused to a 2μm diam. spot, and, with care, quantitative results may be obtained. Measurements from a large specimen face gave the carbon content as 8 ± 1 at.%, with some variability from place to place on the surface examined.

Although no studies of lattice parameters *vs* composition across the boron carbide phase field have been published, Robson (1958) in his doctoral dissertation gave these variations for a series of eight analyzed compositions ranging from 9 to 25 at. % C. His parameter *vs* composition functions are in substantial agreement with our data (Fig. 3) for the specimen series described in § II if our chemically analyzed carbon contents are

* Probable random errors in this analysis are difficult to assess, and to my knowledge replicate analyses were not performed owing to the small amount of material available. A standard deviation of $\pm 10\%$ of the analyzed value might reasonably be assumed.

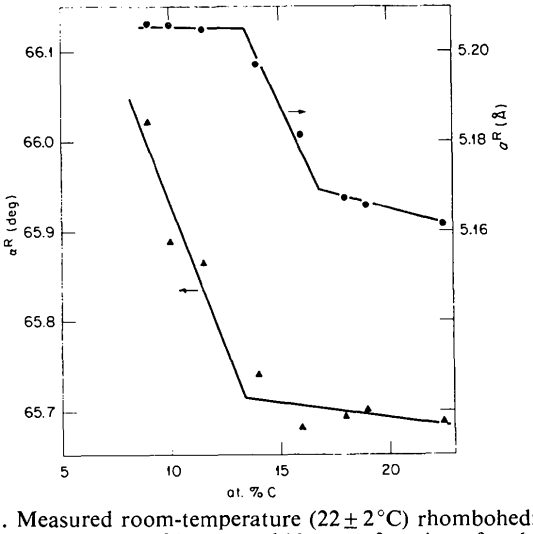

Fig. 3. Measured room-temperature (22 ± 2°C) rhombohedral lattice parameters of boron carbides as a function of carbon content for the series of samples described in § II. Standard deviations in the parameters are of the same order as the size of the symbol plotted. Compositions are those given by bulk chemical analysis except for the three lowest carbon contents where ion microprobe results have been used. Expected errors in the compositions are ± 1 at. % C. Straight-line sections through the data points have been drawn by eye and have no mathematical significance.

Table 2. *Structural parameters of refined trial model FM*

Least-squares standard errors in the last significant figure are given in parentheses.

Occupational, positional, and anisotropic thermal parameters for all atoms. Fixed or constrained values have no error indicated. Parameters β_{ij} appear in temperature-factor expressions of the form $\exp(-h^2\beta_{11} - k^2\beta_{22} - l^2\beta_{33} - 2hk\beta_{12} - 2hl\beta_{13} - 2kl\beta_{23})$. The mass per rhombohedral cell is computed from the occupation parameters and usual atomic weights.

Position	Atom	Parameter	Model FM
18(*h*)	B(1)	Occ.	1·0
		x	−0·16378 (9)
		z	0·35934 (6)
		β_{11}	0·00379 (8)
		β_{33}	0·00075 (2)
		β_{12}	0·00179 (9)
		β_{13}	−0·00016 (2)
18(*h*)	B(2)	Occ.	1·0
		x	−0·10709 (9)
		z	0·11354 (7)
		β_{11}	0·00475 (9)
		β_{33}	0·00060 (2)
		β_{12}	0·0024 (1)
		β_{13}	0·00005 (2)
3(*b*)	B(3)	Occ.	0·742 (5)
		β_{11}	0·0055 (3)
		β_{33}	0·00092 (6)
6(*c*)	C(4)	Occ.	0·742
		z	0·3816 (1)
		β_{11}	0·0029 (1)
		β_{33}	0·00088 (5)
6(*c*)	B(5)	Occ.	0·259
		z	0·4146 (4)
		β_{11}	0·0058 (6)
		β_{33}	0·0008 (2)
36(*i*)	B(6)	Occ.	0·0431
		x	0·264 (2)
		y	0·051 (3)
		z	0·501 (2)
		β_{11}	0·008 (3)
		β_{22}	0·039 (9)
		β_{33}	0·0004 (3)
		β_{12}	0·014 (4)
		β_{13}	0·000 (1)
		β_{23}	0·001 (2)
		Mass/rhomb. cell (a.m.u.)	166·75 (4)

shifted to higher values for the more boron-rich specimens. Extrapolation of Robson's data suggests a B:C ratio of 11:1 (8·3 at.% C) for the lattice parameters reported in § III.

On the basis of all relevant data exclusive of the structure analysis, the average carbon content of the carbide phase is judged to be 8 ± 1 at.% C. The independent composition-sensitive measurements (density, structure analysis, microprobe analysis) on the fragment selected from the bulk specimen are thus self-consistent within one or two standard deviations of each experiment.

VI. Discussion of results

The crystal structure

Interatomic distances and angles between neighboring atoms, computed from the final parameters of model FM with the z coordinate of atom B(6) taken as $\frac{1}{2}$ for simplicity, are given in Table 3. Drawings of major structural entities in Fig. 4 help identify atoms designated in this table. A view of the coordination of six icosahedra about a [CBC] chain and about a [B_4] group is shown in Fig. 5. It is convenient to discuss the average structure in terms of each of the major entities.

Table 3. *Interatomic distances and angles from model FM**

Least-squares standard errors in the last significant figure are given in parentheses. Angles fixed by symmetry have no indicated error. Refer to Fig. 4 for the atom-numbering scheme used under 'Example'; with the centre of the icosahedron of unprimed atom numbers as origin, centers of icosahedra of singly, doubly, and triply primed atom numbers are translated by $\mathbf{a}_1+\mathbf{a}_2, \mathbf{a}_1$, and $\mathbf{a}_1/3+2\mathbf{a}_2/3-\mathbf{c}/3$, respectively, where all vectors are in the hexagonal system. The number of equivalent distances or angles per structural unit being considered (*A*–icosahedron, *B*–[CBC] chain, *C*–[B_4] group) is listed under 'Number'.

A. Intra- and intericosahedral contacts

	Example	Number	
B(2)–B(2)‴	6–1‴	6	1·744 (2) Å
B(1)–B(1)	10–9	6	1·781 (1)
B(1)–B(2)	10–1	6	1·802 (1)
B(1)–B(2)	9–1	12	1·805 (1)
B(2)–B(2)	1–2	6	1·822 (2)
B(1)–B(1)–B(1)	9–10–11	6	108·15 (5)°
B(1)–B(1)–B(2)	9–10– 1	12	60·49 (4)
B(1)–B(1)–B(2)	9–10– 4	12	60·32 (4)
B(1)–B(1)–B(2)	9–10– 5	12	108·80 (4)
B(1)–B(2)–B(1)	9– 1–10	12	59·18 (3)
B(1)–B(2)–B(1)	9– 1–11	6	106·09 (6)
B(2)–B(2)–B(1)	2– 1–10	12	107·15 (3)
B(2)–B(2)–B(1)	2– 1– 9	12	107·12 (3)
B(2)–B(2)–B(1)	3– 1– 9	12	59·69 (3)
B(2)–B(1)–B(2)	4–10– 1	12	109·80 (6)
B(2)–B(1)–B(2)	4–10– 5	6	60·63 (6)
B(2)–B(2)–B(2)	1– 2– 3	6	60·00
B(1)–B(2)–B(2)‴	7– 6– 1‴	6	117·88 (8)
B(1)–B(2)–B(2)‴	8– 6– 1‴	12	121·18 (4)
B(2)–B(2)–B(2)‴	4– 6– 1‴	12	125·58 (5)
Center–B(2)–B(2)‴	0– 6– 1‴	6	175·13 (9)

B. [CBC] Intrachain and chain-icosahedra contacts

C(4)–B(3)	13–14	2	1·438 (1) Å
B(1)–C(4)	12–13	6	1·632 (1)
C(4)–B(3)–C(4)	13–14–15	1	180·00°
B(1)–C(4)–B(3)	12–13–14	6	99·54 (5)
B(1)–C(4)–B(1)″	12–13– 8″	12	117·31 (3)
B(1)–B(1)–C(4)	11–12–13	12	121·32 (2)
B(2)–B(1)–C(4)	2–12–13	6	119·44 (7)
B(2)–B(1)–C(4)	5–12–13	12	121·67 (6)
Center–B(1)–C(4)	0–12–13	6	178·80 (7)

Table 3 (*cont.*)

C. [B_4] Intragroup and group-icosahedra contacts

B(5)—B(6)	16–17	4	1·72 (2) Å
B(5)—B(5)†	16–18	1	2·07 (1)
B(6)—B(6)†	17–19	1	2·75 (1)
B(1)—B(5)	12–16	6	1·743 (2)
B(2)—B(6)	6–17	2	1·65 (1)
B(1)—B(6)	12–17	2	1·80 (2)
B(2)‴–B(6)	1‴–17	2	1·82 (1)
B(5)—B(6)–B(5)	16–17–18	2	74·1 (5)°
B(1)—B(5)–B(1)″	12–16– 8″	12	106·1 (2)
B(1)—B(5)–B(6)	12–16–17	2	62·5 (5)
B(1)—B(5)–B(6)	12–16–19	2	157·9 (6)
B(1)″–B(5)–B(6)	8″–16–19	2	70·8 (5)
B(1)″–B(5)–B(6)	8″–16–17	2	142·4 (6)
B(1)′—B(5)–B(6)	10′–16–17	2	111·5 (6)
B(1)′—B(5)–B(6)	10′–16–19	2	95·6 (6)
Center–B(1)–B(5)	0–12–16	6	168·1 (2)
B(2)—B(6)–B(5)	6–17–16	2	120 (1)
B(2)—B(6)–B(5)	6–17–18	2	166 (1)
B(1)—B(6)–B(5)	12–17–16	2	59·4 (6)
B(1)—B(6)–B(5)	12–17–18	2	129·5 (7)
B(2)‴–B(6)–B(5)	1‴–17–16	2	142 (1)
B(2)‴–B(6)–B(5)	1‴–17–18	2	111 (1)
B(2)‴–B(6)–B(2)	1‴–17– 6	2	59·9 (3)
B(2)—B(6)–B(1)	6–17–12	2	62·9 (6)
B(2)‴–B(6)–B(1)	1‴–17–12	2	117·3 (7)
Center—B(2)–B(6)	0– 6–17	2	115·7 (6)
Center—B(1)–B(6)	0–12–17	2	110·4 (3)
Center‴–B(2)‴–B(6)	0‴–1‴–17	2	124·0 (5)

* The z parameter of atom B(6) has been equated to $\frac{1}{2}$ for brevity.

† Non-bonded or weakly bonded contacts.

A. Icosahedra – Comparisons of certain intraicosahedral distances, distance ratios, and angles, calculated from model FM and from results for B_4C (LC) are shown in Table 4. Values of ratios and angles for a geometrically ideal icosahedron are also listed. It is evident that icosahedra in the boron-rich phase approach the ideal more closely than those in B_4C. Icosahedra in both structures are slightly elongated in the **c** (hex.) direction, as seen in the low values of the width:height ratios, W[B(1)]:H[B(2)], relative to ideality. Approximating the volume of an irregular icosahedron as proportional to the cube of its average edge (M1), the volume in the boron-rich carbide is about 2·0% greater than that in B_4C. This may be compared with a relative unit-cell volume increase of 3·2% between the same composition limits.

All intraicosahedral distances, except the B(1)–B(2) contacts that lie at an angle to the mirrors, are about 0·02 Å longer in the boron-rich carbide than in B_4C. In detail, these increases correspond to (*a*) dilation of the equilateral triangles formed by B(2) atoms at adjacent

rhombohedral vertices, and (*b*) movement of B(1) equatorial atoms away from the icosahedral mid-plane {ratio H[B(1)]:H[B(2)]}. The first adjustment is probably due to the increased α angle of the rhombohedral unit cell coupled with the structural requirement (Hoard & Hughes, 1967) that icosahedral frameworks keep intericosahedral bond vectors as close as possible to pseudo-fivefold axes (directions from icosahedron centers to vertex atoms). The second adjustment is again probably due to the increased unit-cell dimensions coupled with the same structural requirement applied to bond vectors from equatorial B(1) atoms to C(4) atoms of [CBC] chains of fixed length.

The intericosahedral bond in the boron-rich carbide is also about 0·02 Å longer than that found in B_4C by LC. An important contribution to this expansion (as well as to the expanded intraicosahedral B(2)–B(2) and O–B(2) distances) must arise from elimination of carbon atoms randomly substituted in rhombohedral B(2) sites. Constrained to a mirror plane in the average structure, the intericosahedral bond is inclined toward the hexagonal basal plane by 4·9° from the pseudo-fivefold axis defined by the O–B(2) vector. This misorientation is relatively large compared to the value of 1° for the corresponding bond in B_4C cited by Hoard & Hughes (1967), but it agrees in both magnitude and direction with the 4·79° value computed from LC's parameters.

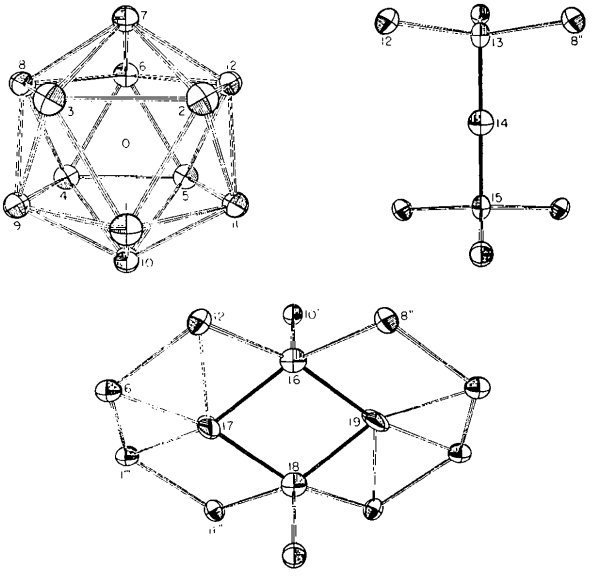

Fig. 4. Drawings of major structural components of model FM. In all cases $\mathbf{a}_1$(hex.) is horizontal and directed to the right, atoms are represented by thermal vibration ellipsoids including 90% probability (2·5 × r.m.s. displacement), and bonds are drawn with arbitrary radii. Top left – an icosahedron viewed along **c**(hex.). The scale of this drawing is about 1·2 times the scale of the other two. Top right – a linear [CBC] chain and the equatorial icosahedral boron atoms to which it bonds. **c**(hex.) is nearly vertical. Bottom – a planar [B_4] group and the icosahedral atoms to which it bonds in one of six possible locations for the pair of B(6) atoms. Orientation of **c**(hex.) is again nearly vertical and intra-group bonds are shown as solid sticks. Primes on numbered atoms in the last two drawings indicate different icosahedra.

Table 4. *A comparison of intraicosahedral distances, distance ratios, and angles for boron-rich (FM) and carbon-rich (LC) boron carbides*

	FM	LC	Number
B(1)–B(1)	1·781 (1) Å	1·7618 (4) Å	6
B(1)–B(2)	1·802 (1)	1·7860 (5)	6
B(1)–B(2)	1·805 (1)	1·8008 (4)	12
B(2)–B(2)	1·822 (2)	1·8062 (6)	6
Mean (M1)	1·803 (1)	1·7911 (4)	
O–B(1)	1·695 (1)	1·6813 (4)	6
O–B(2)	1·734 (1)	1·7252 (4)	6
Mean (M2)	1·715 (1)	1·7032 (4)	
H[B(2)]*	1·379 (1)	1·3743 (3)	
H[B(1)]	0·316 (1)	0·3040 (2)	
W[B(1)]	1·443 (1)	1·4320 (2)	

Ratio	FM	LC	Ideal
M1:M2	1·051 (1)	1·0515 (4)	1·05146
M1:H[B(2)]	1·308 (2)	1·3031(5)	1·32317
M2:H[B(3)]	1·244 (2)	1·2392 (5)	1·25842
H[B(1)]:H[B(3)]	0·229 (1)	0·2212 (3)	0·23607
W[B(1)]:H[B(2)]	1·046 (1)	1·0420 (3)	1·07047

	FM	LC	Ideal	Number
B(1)–O–B(2)	63·39 (4)°	63·23 (1)°	63·435°	6
B(1)–O–B(2)	63·51 (2)	63·814 (8)	63·435	12
B(1)–O–B(1)	63·39 (2)	63·194 (6)	63·435	6
B(2)–O–B(1)	63·39 (5)	63·13 (2)	63·435	6
Mean	63·43 (4)	63·436 (9)	63·435	

* H[B(2)] is defined as z[B(2)] . |**c**(hex.)|, H[B(1)] as $|\frac{1}{3} - z$[B(1)]| . |**c**(hex.)|, and W[B(1)] as $\frac{3}{2}$. $|\frac{1}{3} + x$[B(1)]| . |$\mathbf{a}_1$(hex.)|.

Thermal vibration parameters of icosahedral atoms given in Table 2 are generally larger than those reported by LC. A likely cause for these differences is the altered coordination of icosahedral atoms bonded to [B_4] groups (see below), but they may also reflect contributions of static displacement terms to the intensity losses at Bragg maxima that the least-squares analysis treats as due to thermal vibrations only.

B. [CBC] *chains* – The intrachain B(3)–C(4) distance and the B(1)–C(4)–B(3) and B(1)–C(4)–B(1′) angles given in Table 3 are only slightly changed from their values in B_4C (1·4325 Å, 99·92°, and 117·10°, respectively, from LC's parameters). The small magnitudes of the angular differences in spite of comparatively large unit-cell parameter variations are a consequence of displacements of B(1) atoms away from icosahedral mid-planes in the boron-rich phase. On the other hand, the B(1)–C(4) contacts reflect the cell parameter variations and the distance in Table 3 is about 0·03 Å longer than the 1·6058 Å value computed from LC's parameters. Thermal vibration parameters of [CBC] chain atoms are relatively similar in the two structures.

C. [B_4] *groups* – The existence of these groups is the most important result of the structural analysis presented here. Their configuration seems to be unique

among previously reported entities in higher borides and boron allotropes.

To more fully describe the group, the following assumptions which cannot be confirmed by the existing data, but which seem reasonable, are made:

(*a*) The bridge atoms, B(6), are located at opposite ends of a vector bisected by the threefold axis that exists in the average structure, giving a planar [B_4] group.

(*b*) Since there are six such vectors that are symmetrically equivalent about each center, the bridge atoms of a given group occupy the ends of one of the six at random.

Terminal B(5) atoms form bonds with three equatorial B(1) atoms at a distance of 1·743 Å and with the two bridge atoms of the group at a distance of 1·72 Å. Angles about B(5) atoms involving only bonded B(1) atom neighbors are more nearly tetrahedral than the corresponding angles about C(4) atoms of [CBC] chains. The distance between terminal atoms of a given group is about 0·2 Å larger than the average intraicosahedral boron–boron contact and any chemical bonding between the two must be weak.

In addition to two 1·72 Å bonds to terminal B(5) atoms, each B(6) bridge atom forms one short and two long bonds to icosahedral atoms. As may be seen in Fig. 5, average coordinates of any of the 12 randomly occupied B(6) sites tend to minimize the distance between that B(6) atom and a rhombohedral B(2) atom of an adjacent icosahedron. The corresponding B(6)–B(2) distance of 1·65 Å is among the shortest reported for boron–boron links in icosahedral frameworks; it approaches the 1·624 Å intericosahedral bonds found in β-rhombohedral boron (Hoard, Sullenger, Kennard & Hughes, 1970) and in YB_{66} (Richards & Kasper, 1969), and the 1·60 Å bisphenoidal boron bonds found in α-tetragonal boron (Hoard, Hughes & Sands, 1958).

Of the two longer links from B(6) to icosahedral atoms, one involves an equatorial B(1) atom in the icosahedron containing the closely bonded B(2) atom. The second involves the rhombohedral atom forming an intericosahedral link to the closely bonded B(2) atom (see Fig. 5). The B(1) atom is nearly coplanar with the [B_4] group, while the more loosely bonded B(2) atom is somewhat removed from this plane.

The only other reported occurrence of regular chain replacement in an icosahedral boron compound is orthorhombic aluminum boron carbide, $C_8Al_{2\cdot1}B_{51}$ (Perrotta, Townes & Potenza, 1969). This phase, sometimes given the composition C_4AlB_{24} (Will, 1969), has a hexagonal rather than a cubic stacking sequence of (B_{12}) icosahedra, and has [CBC] chains as intericosahedral linking components with a random probability of about three-fourths. The other one-fourth of the linking components are [C–Al–C] groups in which aluminum atoms occupy one of four symmetrically equivalent sites in a plane normal to the C–C vector. Statistical distributions of boron atoms in channels formed by icosahedra and nonicosahedral cages have been reported for YB_{66} (Richards & Kasper, 1969).

The phase diagram

The crystal structure of boron-rich boron carbide proposed here demonstrates that carbon depletion

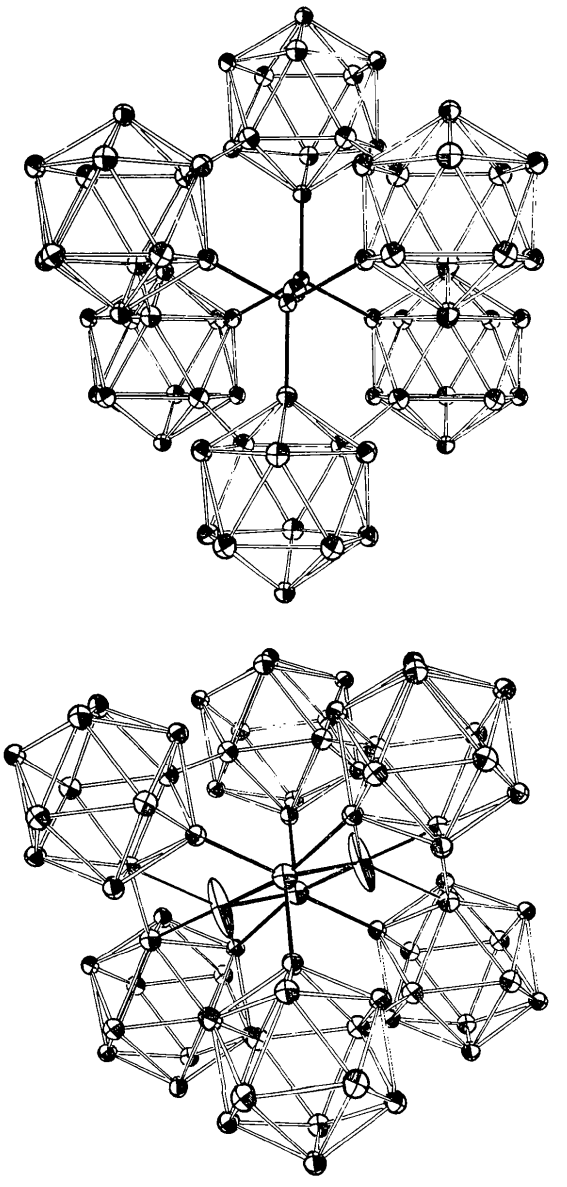

Fig. 5. Drawings of the six icosahedra coordinated about a [CBC] chain (top) and about a [B_4] group in one of its possible orientations (bottom) prepared with parameters of model FM. In both cases $\mathbf{a}_2$(hex.) is nearly vertical and **c**(hex.) is nearly normal to the page. Atoms are represented by thermal vibration ellipsoids including 90% probability and bonds are drawn with arbitrary radii. Thick solid bonds from B(6) atoms are used for the three shortest interatomic contacts; thinner open bonds delineate the two longer B(6)–B(1) and B(6)–B(2) contacts.

below (B_{12}) [CBC] is accomplished neither by additions of significant numbers of interstitial atoms in the sites suggested by Clark & Hoard (1943), nor by replacement of chains by voids so as to approach the α-rhombohedral boron structure (Decker & Kasper, 1959). Rather, there is a replacement of chains by a new linking component consisting of four boron atoms whose effective 'width' [*i.e.*, their dimension perpendicular to **c** (hex.)] is clearly greater than that of the [CBC] chains.

One may attempt to rationalize the changes in lattice parameter with composition observed as a part of the present work in terms of the structural entities likely to be present in sensible numbers at a given carbon content. At the carbon-rich extreme these entities would be ($B_{11}C$), (B_{12}), and ($B_{10}C_2$) icosahedra and [CBC] chains. As carbon is removed from the structure, concentrations of carbon-substituted icosahedra decrease until the 'stoichiometric' (B_{12}) [CBC] structure is achieved. Little effect on the rhombohedral unit-cell angle should be observed in this depletion but the cell edge should increase since intericosahedral C–B bonds are replaced by longer B–B contacts. On further carbon depletion, [CBC] chains are replaced by [B_4] groups and a likely consequence should be an increase in unit cell angle with little effect on cell edge. As Fig. 3 shows, these anticipated trends are found.

One may also ask if reasons for limiting carbon concentrations of the boron carbide phase are indicated by the proposed crystal structure. Three structure-sensitive contributions to the overall free energy of the system at any carbon content can be described. These are: (*a*) stabilization gained by a decrease in electronic energy of the system, (*b*) stabilization gained by the increase in entropy of the system, and (*c*) destabilization suffered by the increase in the lattice-strain energy of the system due to random atom or entity substitution. Changes in one or more factors may account for the observed solubility limits.

Longuet-Higgins & Roberts (1955) showed that a regular (B_{12}) icosahedron requires 38 valence electrons for optimal internal and external bond formation. Hoard & Hughes (1967) applied this criterion to compositions of boron carbides and isostructural boron compounds, but with inconsistent success. The extent to which changes in bond energies may dictate the boron-rich composition limit of boron carbide is rendered more ambiguous by the discovery of a new linking component whose bonding electron requirements are not known.

Entropies of ensembles of equivalent states of a given boron carbide containing appropriate numbers of icosahedral and linking component entities would seem to be more easily calculable. Qualitatively, one might expect stabilization due to entropy effects in boron carbides to be minimal near 'stoichiometric' (B_{12}) [CBC] and to rise as carbon atoms randomly enter rhombohedral vertices of icosahedra, or as [B_4] groups randomly replace [CBC] chains.

The simple entropy concepts outlined above are complicated by the smaller statistical weights that must be given to states in which significant lattice strains are generated by special atom configurations (*e.g.*, C–C intra- or intericosahedral bonds, accommodation of [B_4] groups). Such strains may indeed be the dominant effect in determining carbon solubility limits at both extremes of the boron carbide phase. Their accumulation in a structure in which [B_4] entities were numerous but not predominant could raise the free energy to the point of thermodynamic instability. No compensating stabilization due to the growing numbers of [B_4] groups could be envisioned since (B_{12}) [B_4] is not a known boron allotrope.

V. Computer programs used

Preliminary corrections to the data were made with a program *DATASORT* written by H. A. Levy and G. M. Brown but not formally reported. Structure factor, least-squares refinements were made with a modified version *XFLS*, accession number 389 in the *World List of Crystallographic Computer Programs* (Shoemaker, 1966). Interatomic distances and angles were computed with program *ORFFE* (accession number 363) and structural drawings were prepared with a modification of program *ORTEP* (accession number 387). Fourier series were summed and plotted with a program *FORDAPER* written by G. D. Brunton but not formally reported.

I am grateful to J. P. De Luca who prepared the materials studied, to H. A. Levy who permitted me to perform the diffraction experiments with his automated diffractometer, and to J. F. McLaughlin and S. S. Cristy who performed the ion microprobe analyses. The manuscript was constructively criticized by B. S. Borie, J. Brynestad, and H. A. Levy.

References

BROWN, G. M. & CHIDAMBARAM, R. (1969). *Acta Cryst.* B**25**, 676–687.

CLARK, H. K. & HOARD, J. L. (1943). *J. Amer. Chem. Soc.* **65**, 2115–2119.

CROMER, D. T. & WABER, J. T. (1964). *Scattering Factors Computed from Relativistic Dirac–Slater Wave Functions.* Report LA-3056, Los Alamos Scientific Laboratory, Los Alamos, New Mexico, U.S.A.

DECKER, B. F. & KASPER, J. S. (1959). *Acta Cryst.* **12**, 503–506.

ELLIOTT, R. P. (1961). *The Boron–Carbon System.* Report ARF 2200-12, Armour Research Foundation, Illinois Institute of Technology, Chicago, Illinois, U.S.A.

EVANS, C. A. JR (1972). *Anal. Chem.* **44**, 67A–80A.

HOARD, J. L. & HUGHES, R. E. (1967). In *The Chemistry of Boron and Its Compounds*, edited by E. L. MUETTERTIES, pp. 25–154. New York: John Wiley.

HOARD, J. L., HUGHES, R. E. & SANDS, D. E. (1958). *J. Amer. Chem. Soc.* **80**, 4507–4515.

HOARD, J. L., SULLENGER, D. B., KENNARD, C. H. L. & HUGHES, R. E. (1970). *J. Solid State Chem.* **1**, 268–277.
LARSON, A. C. (1974). Private communication.
LARSON, A. C. & CROMER, D. T. (1972). *Reexamination of the Crystal Structure of* B_4C, abstract IV-1, Ninth International Congress of the International Union of Crystallography, Kyoto, Japan, August 26–September 7, 1972. *Acta Cryst.* A**28**, S53.
LONGUET-HIGGINS, H. C. & ROBERTS, M. DE V. (1955). *Proc. Roy. Soc.* A**230**, 110–119.
PEROTTA, A. J., TOWNES, W. D. & POTENZA, J. A. (1969). *Acta Cryst.* B**25**, 1223–1229.
RICHARDS, S. M. & KASPER, J. S. (1969). *Acta Cryst.* B**25**, 237–251.
ROBSON, H. E. (1958). Doctoral dissertation, Univ. of Kansas, unpublished.
SANDS, D. E. & HOARD, J. L. (1957). *J. Amer. Chem. Soc.* **79**, 5582–5583.
SHOEMAKER, D. P. (1966). *World List of Crystallographic Computer Programs*, 2nd ed. Utrecht: Ooesthoek.
WALTERS, K. L. & GREEN, J. L. (1970). In *Quarterly Status Report on the Advanced Plutonium Fuels Program, October* 1, 1970 – *December* 31, 1970, pp. 14–16. Report LA-4595-MS, Los Alamos Scientific Laboratory, Los Alamos, New Mexico, U.S.A.
WILL, G. (1969). *Acta Cryst.* B**25**, 1219–1222.
ZHDANOV, H. S. & SEVAST'YANOV, N. G. (1941). *C. R. Acad. Sci. USSR*, **32**, 432–434.

Acta Cryst. (1975). B**31**, 1806

The Crystal Structure of an Intermediate Scapolite – Wernerite

BY S. B. LIN* AND B. J. BURLEY

Department of Geology, McMaster University, Hamilton, Ontario, Canada

(*Received* 14 *January* 1974; *accepted* 3 *February* 1975)

The crystal structure of a scapolite (52% M) with strong superlattice reflexions ($h+k+l=$ odd) has been determined in space group $P4_2/n$. The three-dimensional intensity data were collected with a normal beam single-crystal diffractometer using Mo $K\alpha$ radiation. Two quantitative relationships were obtained, *viz.* (1) the exponential relationship between the intensity ratio $r(r=\sum I_{h+k+l=\text{odd}}/\sum I_{h+k+l=\text{even}})$ and the atomic displacement from the imaginary mirror plane being consistent with the space group $I4/m$; (2) the linear relationship between the above intensity ratio and the difference of Al occupancy between T(2) and T(3) sites. The horizontal disposition of the disordered CO_3 groups in this scapolite is the same as those present in others, but the vertical disposition is different. In this scapolite the planar CO_3 groups are essentially tilted from the (001) plane.

Introduction

Scapolites form a solid solution series between marialite ($Na_4Al_3Si_9O_{24}Cl$) and meionite [$Ca_4Al_6Si_6O_{24}(CO_3.SO_4)$] and the basic structure has been ascertained (Deer, Howie & Zussman, 1963). The pseudo-body-centred structure of marialitic scapolite has been established by Lin & Burley (1973*a*). However, it still needs further confirmation by more systematic investigations because a precise determination of a pseudosymmetric structure is difficult owing to the much weaker extra reflexions and the high correlation among the structural parameters. Therefore, a gem scapolite of Tsarasaotra, Madagascar (specimen XL) was selected for further study for the following reasons.

(*a*) The extra, weak reflexions ($h+k+l=$ odd) of this intermediate scapolite are much stronger than those displayed by the marialitic scapolite. The relationship between the structural distortion and the intensity of the weak $h+k+l=$ odd reflexions can be further examined.

(*b*) Scapolite XL has an intermediate composition (52% M)† with more Al atoms than the marialitic scapolite, and it should provide information for the understanding of the relationship between the distribution of Al and the intensity of the $h+k+l$ odd reflexions.

(*c*) Since the scapolite XL contains chlorine and carbonate in about equal amounts, the internal strain caused by $Cl \rightleftharpoons CO_3$ substitution will become profound, and a corresponding complexity in the environment around the site occupied by Cl and CO_3 is expected.

Experimental

The space group of the scapolite XL is $P4_2/n$ with nearly three times stronger ($h+k+l=2n+1$) reflexions than those of scapolite ON8 (Lin & Burley, 1973*a*).

* Present address: Department of Geology, National Taiwan University, Taipei, Taiwan, China.

† Where % M = (number of Ca, Sr, Fe, Mn, Mg atoms per unit cell/number of Na, K, Ca, Sr, Fe, Mn, Mg atoms per unit cell) × 100.